# Crystal Structure of a *cis*-Azo-*N*-oxide (2,3-Diazabicyclo[2.2.2]oct-2-ene *N*-Oxide); Analysis by PRDDO and STO-3G MO Calculations *

S. LARSEN and J. P. SNYDER

Chemistry Departments IV and II, The H. C. Ørsted Institute, Universitetsparken 5, DK-2100 Copenhagen Ø, Denmark

The crystal structure of the title compound has been determined by X-ray diffraction methods using 846 observed reflections measured on an automatic diffractometer. The unit cell dimensions are $a = 9.732(2)$ Å; $b = 6.719(1)$ Å; $c = 10.211(2)$ Å; $\beta = 102.54°$, and the space group is $P2_1/n$, $Z = 4$. The final least-squares refinement gave a unit weighted residual of 0.037. The structure shows that the molecule has a highly symmetrical hydrocarbon backbone and a planar but distorted CNN(O)C moiety. The CNN and CNN(O) angles are 119.1 and 109.8°, respectively, while rCN = 1.491 Å and rCN(O) = 1.507 Å. The C−N and N−N bond lengths are compared to those of the corresponding azoalkane and a bicyclic azo-*N*,*N*'-dioxide. Variations in molecular dimensions along the redox series are discussed in terms of PRDDO and STO-3G Mulliken population analyses and the mechanism for retrocycloaddition of unsaturated azo-*N*-oxides. Finally a short C−H⋯O intermolecular contact distance of 2.45 Å suggests the presence of hydrogen bonding.

Cyclic azoalkanes are of interest as versatile synthetic intermediates [2] and as mechanistic probes.[3,4] In the area of reaction dynamics, the manner in which nitrogen is released from unsaturated azo compounds *1* has drawn considerable attention.[4] Similar studies have been conducted on the corresponding azo-*N*-oxides *2*, which decompose to give hydrocarbon and N_2O.[5] Although both N_2 and N_2O thermal extrusions occur by a concerted, single-step pathway, the energy barrier for loss of N_2 is more than 109 kJmol^{-1} (26 kcal/mol) lower than for the corresponding loss of N_2O.[1,4,5]
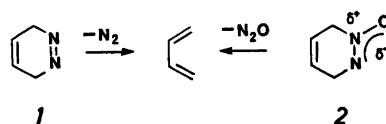
In an attempt to resolve some of the questions raised by the relative energetics of the heteroextrusion reactions, it became expedient to carry out theoretical calculations of the reaction paths. Since no experimental structural information is available for the azo-*N*-oxides, an X-ray analysis for 2,3-diazabicyclo[2.2.2]oct-2-ene *N*-oxide *3* was undertaken. Substrate *3* was chosen in order to make a comparison with the known structure of the azo parent *4*.[6]
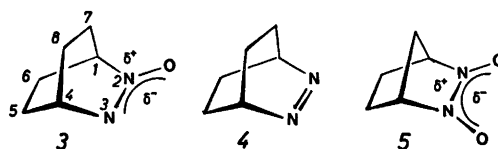
EXPERIMENTAL

Azo-*N*-oxide *3* was prepared as previously described.[7] Recrystallization from ether provided crystals suitable for the X-ray diffraction work. The crystals grow as prismatic needles elongated along [101]. X-Ray diffraction photographs show that they are monoclinic. The space group is uniquely determined to be $P2_1/n$ from the systematically absent reflections.

A single crystal of dimension $0.39 \times 0.18 \times 0.13$ mm^3 was selected for the data collection and for the accurate determination of unit cell parameters using Cu$K\alpha$ radiation from a graphite monochromator. The setting angles for 24 reflections were optimized automatically on a

Picker FACS-1 diffractometer and used in a least-squares refinement of the unit cell parameters and the orientation matrix. The intensity data were collected by operating the diffractometer in the $\theta - 2\theta$ scan mode at a rate of 2°/min in 2θ. The scan range was symmetrical and increased by 2θ in accord with the expression $\Delta 2\theta_{sc} = 3°.6 + 0.286 \tan \theta$. Background counts were made for 20 s at each end of the scan range.

The intensities of three standard reflections were measured after every 40 reflections. These measurements showed that no deterioration and misalignment of the crystal had occurred during data collection. Reflections in the hemisphere $(h \geqslant 0)$ with 2θ between 2.4 and 125° were measured. The intensities of symmetry related reflections were averaged and the data set was corrected for Lorentz and polarization effects but not for absorption. Of the 950 independent reflections obtained 846 were classified as observed with $I/\sigma(I) > 2.0$.

During the crystallographic calculations, use was made of the following computer programs: The Vanderbilt System [8] for all diffractometer operations, a data reduction program of local origin, ORTEP II [9] for the illustrations, MULTAN [10] for the structure solution, the X-Ray System [11] for the refinement and the crystal structure analysis and the program THMB [12] for the analysis of thermal parameters.

For carbon, nitrogen and oxygen the atomic scattering factors of Cromer and Mann [13] were used. For hydrogen the values of Stewart, Davidson and Simpson [14] were employed.

CRYSTAL DATA

2,3-Diazabicyclo[2.2.2]oct-2-ene N-oxide $C_6H_{10}N_2O$; $M = 126.16$. Monoclinic, $a = 9.732(2)$ Å, $b = 6.719(1)$ Å, $c = 10.211(2)$ Å, $\beta = 102.54°$; $V = 650.86$ Å^3; $d_{cal} = 1.287$ g/cm^3; $Z = 4$. $\mu(CuK\alpha) = 7.00$ cm^{-1}, $F(000) = 272$. Systematically ab-

sent reflections: $h0l$ when $h+l$ odd, $0k0$ when k odd. Spacegroup $P2_1/n$.

STRUCTURE DETERMINATION AND REFINEMENT

The structure was solved by means of the program system MULTAN.[10] A standard run gave starting coordinates for all non-hydrogen atoms. The structure was refined by the method of least squares, minimizing $\sum w(|F_o| - k|F_c|)^2$ and using the 846 observed reflections. The scale factor and the positional and anisotropic thermal parameters for the heavier atoms were refined by the method of least squares. Convergence was obtained at a surprisingly high R value of 0.11. A difference Fourier calculated after this refinement showed ten peaks significantly above the noise level where one would expect the hydrogen atoms of the molecule to be located. When the positional and individual isotropic thermal parameters for the hydrogen atoms were included in a unit weighted refinement, the R-value decreased from 0.11 to 0.040 in 3 cycles. During the final cycles of refinement, weights of the form $w = (0.36 + 2.6\sigma(F)^2 - 0.0004F^2)^{-1}$ were used. The numerical values in this expression were derived as described by Nielsen.[15] After convergence of the refinement the maximum shift for the parameters was 0.060. The unit weighted and weighted residuals were both 0.037.

The final atomic parameters are listed in Tables 1 and 2. A list of observed and calculated structure amplitudes may be obtained upon request from the authors.

Table 1. Final fractional coordinates and thermal parameters, u_{ij}, (in units of Å$^2 \times 10^{-4}$) for the heavier atoms. The estimated standard deviations are given in parenthesis. The labelling corresponds to *3*. The expression for the temperature factor is exp $\{-2\pi^2(u_{11}h^2a^{*2} + u_{22}k^2b^{*2} + u_{33}l^2c^{*2} + 2u_{12}hka^*c^* + 2u_{23}klb^*c^*)\}$.

Atom	x	y	z	u_{11}	u_{22}	u_{33}	u_{12}	u_{13}	u_{23}
O1	0.8173(2)	0.8661(3)	0.5021(2)	635(10)	1195(15)	533(10)	−22(9)	−83(8)	377(10)
N2	0.8767(2)	0.7755(3)	0.6076(2)	399(10)	689(11)	375(9)	1(8)	−10(8)	105(10)
N3	0.8168(2)	0.6383(3)	0.6560(2)	455(10)	655(11)	574(11)	−120(8)	17(9)	89(9)
C1	1.0219(2)	0.8367(3)	0.6782(2)	417(11)	620(13)	463(12)	−109(10)	34(10)	171(10)
C7	1.1134(2)	0.6529(4)	0.6853(3)	436(13)	955(18)	491(14)	66(12)	93(12)	−17(13)
C8	1.0452(3)	0.4849(4)	0.7476(3)	685(16)	539(14)	607(16)	93(12)	5(13)	−26(12)
C4	0.9107(2)	0.5636(3)	0.7807(2)	508(12)	535(12)	553(14)	−91(10)	53(11)	179(10)
C5	0.9441(3)	0.7327(4)	0.8810(2)	616(15)	719(15)	419(12)	87(12)	122(12)	92(11)
C6	1.0104(3)	0.9005(3)	0.8182(2)	616(15)	502(13)	540(13)	−7(11)	5(12)	−12(10)

Table 2. Positional parameters and isotropic temperature factors for the hydrogen atoms. The temperature factors are exp $\{-8\pi^2 U \sin^2 \lambda/y^2\}$. Standard deviations are in parenthesis.

Atom	x	y	z	$u \times 10^2$ $\mathrm{\AA}^2$
H1	1.049(2)	0.939(3)	0.629(2)	5.9(6)
H71	1.124(2)	0.617(3)	0.599(2)	8.4(8)
H72	1.208(2)	0.690(3)	0.740(2)	7.4(7)
H81	1.107(2)	0.437(4)	0.832(2)	8.5(8)
H82	1.023(2)	0.378(4)	0.684(2)	8.2(7)
H4	0.860(2)	0.460(3)	0.814(2)	6.4(6)
H51	0.856(2)	0.774(3)	0.905(2)	7.7(7)
H52	1.013(2)	0.685(3)	0.959(2)	7.2(7)
H61	1.110(2)	0.929(3)	0.869(2)	6.8(7)
H62	0.955(2)	1.015(4)	0.813(2)	7.5(7)

Table 3. Bond lengths and corrected bond lengths (Corr) with estimated standard deviations.

Bond	$r/\mathrm{\AA}$	Corr/$\mathrm{\AA}$	Bond	$r/\mathrm{\AA}$
C1–N2	1.259(2)	1.270	H1–C1	0.92(2)
N2–N3	1.250(3)	1.266	H71–C7	0.94(3)
C1–N2	1.494(2)	1.507	H72–C7	0.99(2)
C1–C7	1.515(3)	1.532	H81–C8	0.99(2)
C7–C8	1.519(4)	1.538	H82–C8	0.96(2)
C8–C4	1.518(4)	1.535	H4–C4	0.96(2)
C4–C5	1.515(3)	1.534	H81–C5	0.98(2)
C4–N3	1.479(3)	1.491	H52–C5	0.98(2)
C5–C6	1.512(4)	1.530	H61–C6	1.01(2)
C6–C1	1.520(3)	1.538	H62–C6	0.94(2)

DESCRIPTION AND DISCUSSION OF THE STRUCTURE

The molecular structure is shown in Fig. 1. Bond lengths are listed in Table 3; bond angles and dihedral angles, in Table 4.

The overall structure of *cis*-azo-*N*-oxide *3* may be regarded as composed of two fragments. The hydrocarbon backbone is best described as an undistorted boat cyclohexane characterized by the C_{2v} point group. The hetero unit, on the other hand, is planar but severely distorted within the C_1NNC_4 plane accounting for the unequal CCN bond angles around the bridgehead carbons. The CNN bond angles for *3* are also unequal, the oxidized nitrogen angle expanded by 9° relative to that for nitrogen bearing a lone electron pair. Two acyclic *cis*-azo-*N*-oxides exhibit similar behavior (Δ(CN(O)N – CNN) = 7 – 8°).* *Trans* azoxybenzenes are reported either with equal CNN bond angles [17,18] or with $\angle$CNN > $\angle$CN(O)N.[19,20]

The C4 – N3 bond containing trivalent nitrogen is significantly shorter than the C1 – N2 bond involving tetravalent N(O). This behaviour is shown by certain *trans* aryl azo-*N*-oxides [17,19] and one of the *cis* dialkyl derivatives [16],* but not by others.[18,20] Finally the

---

* The two positional isomers of *cis*-cyclohexylmethyl azo-*N*-oxide have been found by X-ray [16] to exhibit the following bond lengths: CH$_3$N(O): rCN(O)= 1.457 Å, rCN= 1.459 Å, c-C$_6$H$_{11}$N(O): rCN(O)= 1.512 Å, rCN= 1.462 Å.
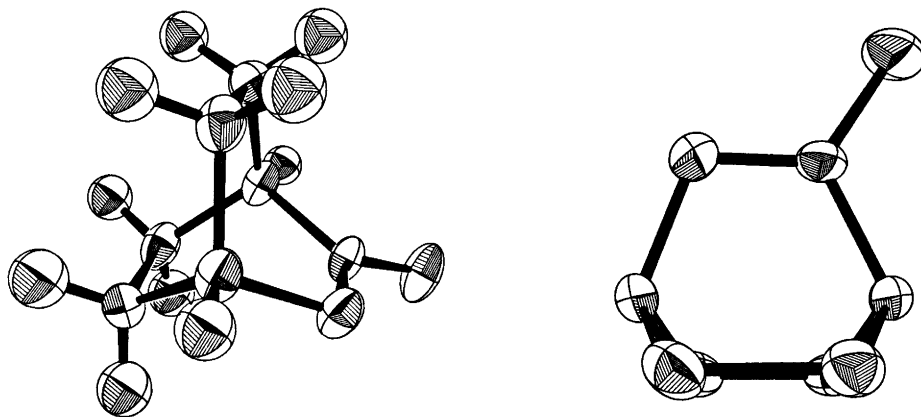

Fig. 1. (a) ORTEP drawing for azo-*N*-oxide *3*. The ellipsoids are scaled to include 25 % probability; (b) Top view of the asymmetric CN(O)NC moiety.

Table 4. Bond angles/deg.

C1-N2-N3	122.0(2)	H1-C1-N2	107(1)
C1-N2-C1	118.9(2)	H1-C1-C7	113(1)
C1-N2-N3	119.1(1)	H1-C1-C6	113(1)
N2-N3-C4	109.7(1)	H71-C7-C1	110(1)
N2-C1-C6	105.8(2)	H71-C7-C3	111(1)
N2-C1-C7	106.4(2)	H72-C7-C1	106(1)
C7-C1-C6	110.5(2)	H72-C7-C8	112(1)
C1-C7-C8	108.6(2)	H81-C8-C7	112(1)
C7-C8-C4	108.3(2)	H81-C8-C4	108(1)
C8-C4-C5	110.3(2)	H82-C8-C7	109(1)
C8-C4-N3	108.9(2)	H82-C8-C4	110(1)
C5-C4-N3	109.0(2)	H4-C4-N3	106(1)
C4-C5-C6	108.6(2)	H4-C4-C8	111(1)
C5-C6-C1	108.5(2)	H4-C4-C5	111(1)
		H51-C5-C4	108(1)
Dihedral angles		H51-C5-C6	112(1)
C1-C6-C5-C4	− 1.1(2)	H52-C5-C4	108(1)
C1-C7-C8-C4	− 0.4(2)	H52-C5-C6	108(1)
C1-N2-N3-C4	+ 0.0(2)	H61-C6-C1	106(1)
C7-C8-C4-C5	− 61.1(2)	H61-C6-C5	112(1)
C8-C4-C5-C6	62.1(2)	H62-C6-C1	110(1)
C8-C4-N3-N2	− 60.3(2)	H62-C6-C5	110(1)

nitrogen oxygen bond distance of 1.270 Å is within the range found for other azoxy compounds (rNO = 1.26 − 1.29 Å).[16−20],**

Comparison of the structure of *3* with the azo parent *4*[6] and the azo-*N*,*N'*-dioxide *5*[22] reveals some interesting gradations along the redox series. In the hydrocarbon part all CC bond lengths in *N*-oxide *3* are virtually the same as those of the corresponding bonds in azo *4*. However, whereas the C_bCCC_b (b = bridgehead) dihedral angles are around 5° for the latter, the same angles are 0° for the *N*-oxide. Carbon-hydrogen bond distances are reasonable (0.92 − 1.01 Å) and similar to those found for *4* (0.95 − 1.04 Å) and *5* (0.94 − 1.01 Å).

As noted above, the heteroatom fragment displays a marked difference in the CN bond lengths, the C1 − N2(O) bond (1.507 Å) elongated relative to C4 − N3 (1.491 Å). Similarly the CN bonds in the *N*,*N'*-azodioxide *5* (1.493 Å average) are longer than those found in (*4*) (1.487 Å). The azoxy NN bond (1.266 Å) is slightly longer than the corresponding distance for (*4*) (1.260 Å), but significantly shorter than rNN in dioxide *5* (1.303 Å). The NO bond distance for *N*-oxide *3* (1.270 Å) is somewhat longer than NO in dioxide *5* (1.260 Å average).

** An exceptionally short NO bond has been found for a cyano-azoxy system.[21]

Finally the NNO bond angle of 122.2° in *3* may be compared to a value of 123.8° in *5*. Some of these variations will be discussed in the following section in connection with theoretical calculations.

MOLECULAR ORBITAL CALCULATIONS

In order to gain insight into the structural changes which occur upon oxidation of (*4*) to the corresponding *N*-oxide and ultimately to the dioxide (*e.g., 5*), MO calculations utilizing the X-ray structures of both substances have been performed. The two basis sets employed were PRDDO[23] and STO-3G.[24]

Bond length variations can be rationalized in terms of the variation of charge distribution. Fig. 2 depicts the calculated charge densities and Mulliken overlap populations for *4* and *N*-oxide *3*. By symmetry the accumulated negative charge at the two nitrogens in *4* is identical. In the *N*-oxide the negative charge density at trivalent nitrogen N3 has increased relative to that of nitrogen in *4*, while it has become positive at N2(O). Accordingly the nearly identical NN bond lengths for *3* and *4* can be viewed as the result of counterbalancing resonance and coulombic effects. In valence bond language the consequence of attaching an oxygen to the azo moiety is pictured in *6*. π-Delocalization over the NNO unit ought to lower the double bond character between the nitrogens, and, to a first approximation, increase the NN bond distance.
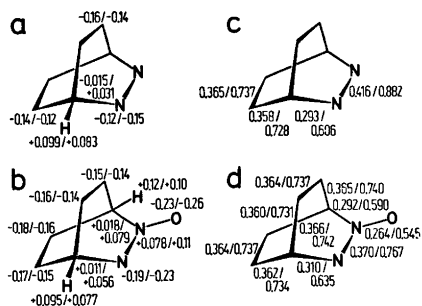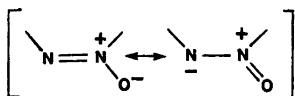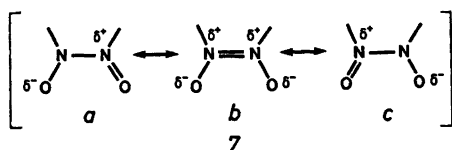

Fig. 2. Charge densities (a), (b) and overlap populations (c), (d) for azo *4* and azo-*N*-oxide *3* from STO-3G/PRDDO calculations. Molecular geometries have been taken from the X-ray determinations.

$$\left[\quad \underset{O^-}{\overset{+}{N}} \quad \longleftrightarrow \quad \underset{O}{\overset{+}{N}} \quad \right]$$
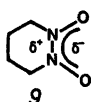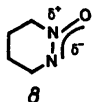
6

Failure to observe significant NN lengthening is appreciated by reference to Fig. 2. The nitrogen-nitrogen overlap population in fact drops by about 12 % in the transition from the azo to azo-*N*-oxide group in agreement with the resonance formulation *6*. However, the loss in covalent bonding is compensated by the electrostatic attraction between oppositely charged atoms N1 and N2 in compound *3*. A breakdown of the charge distribution into σ and π components indicates that the major readjustment of electron density occurs in the σ framework.

A similar analysis accounts for the elongation of the N—N bond by 0.049 Å when an *N*-oxide (*3*) is further oxidized to the corresponding dioxide (*e.g.*, *5*). Here the resonance formalism suggests that the unsymmetrical structures *7a* and *c* should contribute to diminished N—N π character. PRDDO and STO-3G calculations for 2,3-diazacyclohex-1-ene *N*-oxide *8* and the corresponding dioxide *9* result in a drop in the N—N overlap population of around 14 % from *8* to *9*.* However the offsetting opposite charges at nitrogen in *8* are absent in *9* where both nitrogens are positive. Consequently the long NN bond for *5* relative to *3* would appear to arise from a mutually reinforcing set of covalent and electrostatic forces.

$$\left[\quad \underset{\delta^- O}{\overset{\delta^+}{N}}\!\!-\!\!\underset{O}{N} \quad \longleftrightarrow \quad \underset{\delta^- O}{\overset{\delta^+}{N}}\!\!=\!\!\underset{O\,\delta^-}{\overset{\delta^+}{N}} \quad \longleftrightarrow \quad \underset{O}{N}\!\!-\!\!\underset{O\,\delta^-}{\overset{\delta^+}{N}} \quad \right]$$

$$\quad a \qquad\qquad b \qquad\qquad c$$

7

8   **9**

Finally the calculations suggest that the variable NC bond distances in DBO *N*-oxide *3* are influenced both by electrostatic and covalent

---

* Geometries employed for these calculations were obtained by a full MINDO/3 [25],[26] gradient optimization of structures *8* and *9*.

effects but most likely dominated by the latter. The Cl—N2(O) atoms are both positive, while the C4—N3 atoms bear opposite charges. Although this may imply a shorter C4—N3 distance, the absolute magnitude of charge at the C—N centers is significantly less than at NN and the bond distances are considerably longer. Consequently charge distribution can be expected to play a lesser role for changes in *r*CN than for *r*NN. On the other hand, the calculated overlap populations indicate C4—N3 to be a better bond than Cl—N2(O) in agreement with the X-ray result. The "degree of bonding" criterium [27] as defined within the PRDDO framework [23] is corroborative: C4—N3, 0.985; Cl—N2(O), 0.891. Both the latter and the Mulliken overlap populations reflect a somewhat reduced Cl—N2(O) overlap probably caused by orbital shrinkage around the relatively electronegative N2(O).

AZO-*N*-OXIDE FRAGMENTATION

Whatever the underlying cause of the stretching of the Cl—N2(O) bond and the attendant in-plane distortion of the CNN angles in *3*, the structural asymmetry is reproduced by semiempirical computation. A complete geometry optimization for bicyclic azo-N-oxides *10* and *11b* by means of MINDO/3 calculations [5],[26] furnishes the identical quantitative picture (*cf.* Fig. 3).

Of particular note is retention of the pattern of asymmetry at NNO in the unsaturated species *11b*. The X-ray analysis, the fixed geometry PRDDO/STO-3G calculations and the MINDO/3 structures are all completely consistent with our previous results concerning the concerted release of N₂O from *11b* and a series of bicyclic relatives. Activation parameters measured as a function of solvent were interpreted as reflecting a synchronous cleavage of the C—N bonds
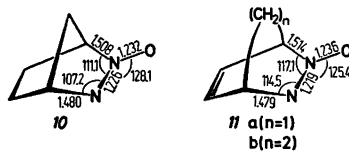
10   *11* a(n=1)
              b(n=2)

Fig. 3. Partial results for the full MINDO/3 geometry optimization for azo-*N*-oxides *10* and *11b* (distances, Å; angles, deg.).

with the C−N(O) bond rupturing slightly faster.[5] Supplementary CNDO/B potential surface calculations for the breakdown of *IIa* are likewise supportive of the asymmetric pericyclic process.[5b] The sum of the experimental and theoretical evidence, then, yields the following picture of the N_2O cycloreversion process. Asymmetry in the C−N bonds for ground states of type *11* is amplified as the molecular complex approaches and traverses the transition state. The perturbation introduced by *N*-oxidation is, however, insufficient to convert the otherwise concerted fragmentation into a two-step biradical transformation.

Questions concerning the enormous rate differential for retrocycloaddition of *1* and *2* still need to be addressed. Differential scanning calorimetry [1] and conventional kinetics studies [5] permit the conclusion that not only is the activation barrier for loss of N_2O from *2* greater that for loss of N_2 from *1*, but the former process is also considerably less exothermic. Thus the shapes of the potential energy surfaces for N_2 and N_2O release are very different. A fuller evaluation of the reasons behind the relative energetics calls for an exploration of the cycloreversions at a level of theory capable of reproducing the known experimental variables.

CRYSTAL PACKING; A POSSIBLE C−H···O HYDROGEN BOND

There are noteworthy differences between the physical properties of azo compound *4* and *N*-oxide *3*. Although the substances' melting points differ by only 12 °C (146−147 and 158−159 °C, respectively [7,28]), the azoalkane is extremely easy to sublime (80 °C/0.2 mmHg) whereas the *N*-oxide requires temperatures 20−30 °C higher and longer times for a comparable vaporization. Greater crystal forces for *N*-oxide *3* relative to azo compound *4* are suggested and reflected further by the dipole moment difference of 1.61 D (3.43 and 5.04 D, respectively, C_6H_6 [29]). The polar NNO units of *3* are, however, separated within the crystal by over 3.5 Å. It seems unlikely that the intermolecular electrostatic interactions alone can account for the differences in crystal forces. Inspection of the intermolecular contact distances reveals the presence of a unique and very short O···H distance. Albeit only neutron diffraction data can provide truly accurate positions for hydrogen atoms, the accuracy of the present data and the unusual contribution of the hydrogen atoms indicated by the 7 % lowering of the *R*-value justify further discussion of this point.
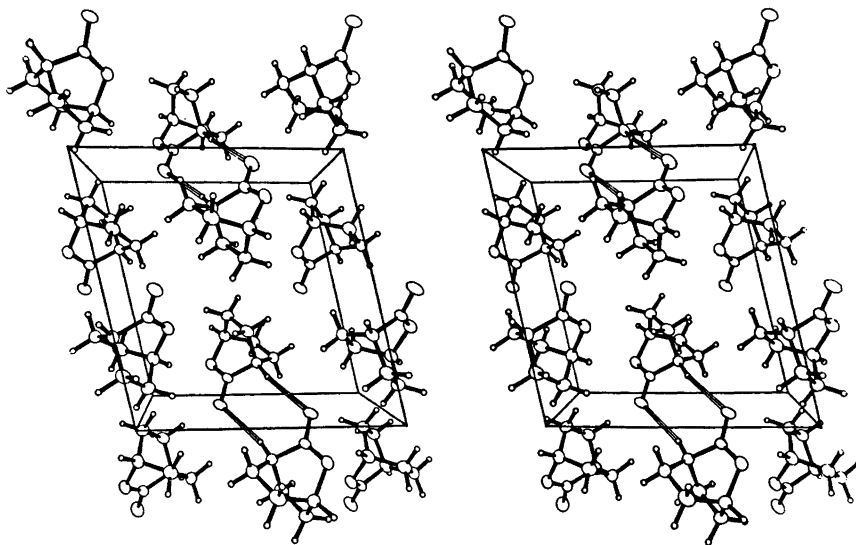

Fig. 4. Stereo pair for azo-*N*-oxide *3* illustrating the packing viewed along the *b* axis.

The O1···H1 distance in question (2.45 Å) is significantly less than the sum of the hydrogen and oxygen van der Waals radii (2.60 Å,[30] 2.72 Å[31]). The corresponding C1−H1···O1 angle is 161°. These observations suggest the presence of the C−H···O bond illustrated in the stereo pair in Fig. 4.

There is appreciable evidence for the existence of this type of bonding in crystals.[32] It has been suggested, for example, that in polyglycine II in addition to the normal interpeptide H-bonds, interpeptide C−H···O=C bonds contribute to conformational properties.[33] Though carbon is not regarded as a particularly electronegative atom, C−H can act as a hydrogen bonding donor, if the whole group carries a net positive charge.[30] Fig. 2 indicates that C1−H1 in azoxy *3* meets this requirement.

In this connection it should be mentioned that the NMR chemical shifts of the bridgehead protons in azo-*N*-oxide *3* (C1−H1 and C4−H4) and a variety of other *cis*-azoxyalkanes are identical. Combined MO and anisotropy calculations have traced this finding to the similar charge densities at the bridgehead hydrogens.[7] Contact distances for O···H4 (2.89 Å) and N2···H4 (2.82 Å) are slightly larger than the sum of the van der Waals radii for these atoms. However, the separations are short enough that they might likewise contribute to the crystal forces of *N*-oxide *3*. Other candidates for a participatory role are O···H72 (2.67 Å), O···H81 (2.71 Å) and N2···H62 (2.85 Å). The STO-3G and PRDDO charges for the latter three protons are +0.085−0.106 and +0.075−0.091 respectively, comparing in magnitude to the values computed for the bridgehead protons.

REFERENCES

1. Oth, J. F. M., Olsen, H. and Snyder, J. P. *J. Am. Chem. Soc. 99* (1977) 8505.
2. *e.g.* Gassman, P. G., Mansfield, K. T., Taylor, G. N. and Wiberg, K. B. *Org Synth. 49* (1969) 1; Heyman, M. L. and Snyder, J. P. *Tetrahedron Lett.* (1973) 2859, and references therein.
3. Bergman, R. G. In Kochi, J. K., Ed., *Free Radicals*, Wiley, New York 1973, Vol. 1, pp. 191−273.
4. Berson, J. A., Olin S. S., Petrillo, E. W., Jr. and Bickart, P. *Tetrahedron 30* (1974) 1639.
5. a. Olsen, H. and Snyder, J. P. *J. Am. Chem. Soc. 96* (1974) 7839; b. Olsen, H. and Snyder, J. P. *Ibid. 99* (1977) 1524.
6. Ottersen, T., Rømming, C. and Snyder, J. P. *Acta Chem. Scand. B 30* (1976) 407.
7. Snyder, J. P., Bandurco, V. T., Darack, F. and Olsen, H. *J. Am. Chem. Soc. 96* (1974) 5158.
8. Lehnert, P. G. *J. Appl. Crystallogr. 8* (1975) 568.
9. Johnson, C. K. *ORTEP: A Fortran Ellipsoid Plot Program for Crystal Structure Illustrations*, Report ORNL-3794, Second Rev., Oak Ridge National Laboratory, Oak Ridge 1970.
10. Declercq, J. P., Germain, G., Main, P. and Woolfson, M. M. *Acta Crystallogr. A 29* (1973) 231.
11. Stewart, J. M. *et al. The X-Ray System 1972*, Technical Report Tr.-192, Computer Science Center, University of Maryland, College Park.
12. Trueblood, K. N. *Abstracts*, Fourth European Crystallographic Meeting, Oxford, England 1977, p. 165.
13. Cromer, D. and Mann, J. B. *Acta Crystallogr. A 24* (1968) 321.
14. Stewart, R. F., Davidson, E. R. and Simpson, W. T. *J. Chem. Phys. 42* (1965) 3175.
15. Nielsen, K. *Acta Crystallogr. A 33* (1977) 1009.
16. Baker, M. S. and Williams, D. E. *Acta Crystallogr. B 33* (1977) 2325.
17. Browning, J., Happer, D. A. R. and Penfold, B. R. *J. Cryst. Mol. Struct. 4* (1974) 187.
18. Cameron, T. S., Cummings, R. J. and Knipe, A. C. *J. Chem. Soc. Perkin Trans. 2* (1976) 802.
19. Krigbaum, W. R. and Barber, P. G. *Acta Crystallogr. B 27* (1971) 1884.
20. Krigbaum, W. R., Chatani, Y. and Barber, P. G. *Acta Crystallogr. B 26* (1970) 97.
21. Viterbo, D., Gasco, G., Serafino, A. and Mortarini, V. *Acta Crystallogr. B 31* (1975) 2151.
22. Prout, K., Stothard, V. P. and Watkin, D. J. *Acta Crystallogr. B 34* (1978) 2602.
23. Halgren, T. A. and Lipscomb, W. N. *J. Chem. Phys. 58* (1973) 1569.

24. Hehre, W. J., Stewart, R. F. and Pople, J. A. *J. Chem. Phys. 51* (1969) 2657.
25. Bingham, R. C., Dewar, M. J. S. and Lo, D. H. *J. Am. Chem. Soc. 97* (1975) 1285, 1294, 1302, 1307.
26. Schmidling, D. *QCPE 10* (1978) 350.
27. Armstrong, D. R., Perkins, P. G. and Stewart, J. J. P. *J. Chem. Soc. Dalton Trans.* (1973) 838.
28. Cohen, S. G. and Zand, R. *J. Am. Chem. Soc. 84* (1962) 586.
29. Ehrbar, U., Larsen, C., Olsen, H. and Snyder, J. P. (H. C. Ørsted Institute). *Unpublished work.*
30. Hamilton, W. C. and Ibers, J.-A. *Hydrogen Bonding in Solids*, Benjamin, New York 1968, pp. 14 – 18.
31. Bondi, A. *J. Phys. Chem. 68* (1964) 441.
32. Suter, D. J. *J. Chem. Soc.* (1963) 1105.
33. Krimm, S., Kuroiwa, K. and Rebane, T. In Ramachandran, G. M., Ed., *Conformation of Biopolymers*, Academic, New York 1967, Vol. 2, p. 439.